

Supporting Information: Aqueous photolysis of benzobicyclon hydrolysate

Katryn L. Williams^{†*}, Richie Kaur[‡], Alexander S. McFall[‡], Jacob Kalbfleisch[§], Joshua J. Gladfelder[§], David B. Ball[§], Cort Anastasio[‡], and Ronald S. Tjeerdema[#]

[†]Now at: Hale Creek Field Station, New York State Department of Environmental Conservation, 182 Steele Ave Extension, Gloversville, NY 12078

[‡]Department of Land, Air, Water Resources, One Shields Avenue, University of California, Davis, CA, 95616

[§]Department of Chemistry and Biochemistry, Physical Science Building Room 216, California State University, Chico, CA, 95929

[#]Department of Environmental Toxicology, One Shields Avenue, University of California, Davis, CA, 95616

*Corresponding author (Tel: 518-773-7138 ext 3002; Email: katryn.williams@dec.ny.gov)

Page S2 – S5: Synthesis of Compound **2** and 3-{3-[2-chloro-4-(methanesulfonyl)phenyl]-3-oxopropanoyl)cyclopentane-1-carboxylic acid

Page S6 – S7: Calculations

Page: Tables

- S8 • Table S1. ε_λ , Φ_λ , photon flux, and j_λ for neutral compound **1**
- S11 • Table S2. ε_λ , Φ_λ , photon flux, and j_λ for anionic compound **1**
- S14 • Table S3. Absorbances and screening factors
- S16 • Table S4. Attenuated j_λ
- S17 • Table S5. TUV calculator input values
- S18 • Table S6. PFAM input values
- S19 • Table S7. Unscreened j_p and $t_{1/2}$ for compound **1** in natural waters

Page: Figures

- S20 • Figure S1. Structure of 3-{3-[2-chloro-4-(methanesulfonyl)phenyl]-3-oxopropanoyl)cyclopentane-1-carboxylic acid
- S20 • Figure S2. Comparison of neutral compound **1** photolysis rates
- S21 • Figure S3. PFAM results (concentration-based)

Page S22: References

Number of tables: 7

Number of figures: 3

Number of pages: 22

Synthesis of 3-(methanesulfonyl)-5a,6,7,8,9,10a-hexahydro-6,9-

methanobenzo[b]cyclohepta[e]pyran-10,11-dione (Compound 2):

To compound **1** (179 mg, 0.5 mmol) in DMF (2 mL) was added K₂CO₃ (69 mg, 0.5 mmol) and the resulting mixture was heated to 100°C for one hour. The reaction was allowed to reach room temperature and stir for 24 hours. H₂O (10 mL) was added to the reaction and the products were recovered via continuous solvent extraction with EtOAc (200mL). Organics were condensed *in vacuo* providing compound **2** as an orange solid (136 mg, 76%). ¹H NMR (300 MHz, DMSO-d₆) δ8.23, 7.97, 3.35, 2.88, 2.18, 1.78.

Synthesis of 3-{3-[2-chloro-4-(methanesulfonyl)phenyl]-3-oxopropanoyl)cyclopentane-1-carboxylic acid:

To a 25 mL 3-necked flask equipped with argon inlet, stir bar, reflux condenser, and dropping funnel was added 4-{1-[2-chloro-4-(methanesulfonyl)phenyl]ethenyl}-morpholino (209 mg, 0.69 mmol; synthesis details below), Et₃N (0.10 mL, 0.69 mmol), and CHCl₃ (3 mL). In a separate flask, methyl (1*S*,3*R*)-3-(chlorocarbonyl)cyclopentane-1-carboxylate (136 mg, 0.69 mmol; synthesis details below) was diluted with 3 mL CHCl₃ and transferred to the dropping funnel via syringe. The dropping funnel and reflux condenser were then equipped with drying tubes (CaCl₂). After heating to 35 °C the dropwise addition of the methyl (1*S*,3*R*)-3-(chlorocarbonyl)cyclopentane-1-carboxylate solution was started and continued over 1.5 hr. Once the addition was completed, the mixture was vigorously stirred at 35 °C for 4.5 hr. An equal part of 6 M HCl was added and refluxed at 60 °C for another 4.5 hr. Once cooled to room temperature, CHCl₃ (3 mL) was added and phases separated. The CHCl₃ was washed with water (5 x 10 mL) and these washings were then combined with the aqueous phase, taken to pH 5-6

with 6 M NaOH, and extracted with CHCl₃ (5 x 10 mL). Consolidation of the CHCl₃ phase and CHCl₃ extractions followed by concentration under reduced pressure afforded a dark orange and viscous oil. Unhydrolyzed methylester was removed by adding equal parts of DCM and water to the crude product and adjusting to pH 9 with NaOH. The DCM phase was then discarded. The remaining aqueous phase was readjusted to pH 1-2 and extracted with DCM. Evaporation under reduced pressure gave a light orange oil which slowly crystallizes to yield 3-{3-[2-chloro-4-(methanesulfonyl)phenyl]-3-oxopropanoyl)cyclopentane-1-carboxylic acid (108 mg, 40%). ¹H NMR (300 MHz, CDCl₃) δ 15.47, 8.03, 7.92, 7.79, 6.08, 3.09, 3.05, 3.89, 2.35-1.92. MS (ESI) m/z: [M + NH₄]⁺ Calculated for C₁₆H₂₁ClNO₆S 390.86; Found 391.

4-{1-[2-chloro-4-(methanesulfonyl)phenyl]ethenyl}morpholino was prepared thusly: To an oven dried 25 mL dual-necked round bottom flask was added morpholine (0.51 mL, 5.9 mmol) and TiCl₄ (0.645 mL, 0.645 mL). In a separate flask, 1-[2-chloro-4-(methylsulfonyl)phenyl]ethane-1-one (0.298 g, 1.28 mmol; synthesis described previously)¹ and toluene (6 mL) were stirred under a mild heat until homogenous and immediately transferred to a dry addition funnel. The mixture of morpholine and TiCl₄ was cooled to 0 °C and 1-[2-chloro-4-(methylsulfonyl)phenyl]ethane-1-one was added dropwise over 20 min. The reaction was then stirred at room temperature for 24 hr and filtered through a celite pad. The pad was then washed with toluene (15 mL). Concentration *in vacuo* offered a viscous yellow residue, which was then dissolved in CHCl₃ (15 mL), to ensure all TiO₂ had been precipitated, and filtered as done previously with CHCl₃ washings (15 mL). Evaporation under reduced pressure afforded 4-{1-[2-chloro-4-(methanesulfonyl)phenyl]ethenyl)morpholino as a bright orange residue in near purity by ¹HNMR (0.2981 g, 77%) and was used without further purification.¹H NMR (300 MHz, CDCl₃) δ 7.98, 7.89, 7.59, 4.37, 4.11, 3.74, 3.10, 2.83.

Synthesis of methyl (1*S*,3*R*)-3-(chlorocarbonyl)cyclopentane-1-carboxylate: To a solution of norbornene (9.40 g, 100 mmol) and RuCl₃ (0.501 g, 2.42 mmol) in 1:1 ethyl acetate: acetonitrile (400 mL) was added a solution of NaIO₄ (87.610 g, 443 mmol) in water (300 mL) slowly and under vigorous stirring. After stirring for 48 hours, the reaction mixture was filtered and phases separated. The aqueous phase was saturated with NaCl and extracted with ethyl acetate (3 x 100 mL). The combined organic layers were then dried over MgSO₄ and evaporated under reduced pressure to afford 13.23 g (84%) of cyclopentane-1,3-dicarboxylic acid as a white crystalline solid and was used without further purification. ¹H NMR (300 MHz, CDCl₃) δ11.06, 2.76, 1.98-1.55.

Cyclopentane-1,3-dicarboxylic acid (12.31 g, 77.8 mmol) was added to 100 mL of glacial acetic acid and refluxed under argon at 120 °C for 45 min. Evaporation of solvent under reduced pressure and subjection to high vacuum for 48 hr yielded 10.6 g of 3-oxabicyclo[3.2.1]octane-2,4-dione as a pale yellow powder (98%) in near purity. ¹H NMR (300 MHz, CDCl₃) δ3.29, 2.29-2.03, 1.80-1.73.

3-oxabicyclo[3.2.1]octane-2,4-dione (4.81 g, 34.3 mmol) was added to dry MeOH (220 mL) and refluxed at 45 °C for 6 hr. Solvent was then evaporated under reduced pressure. The resultant oil was then dissolved in dichloromethane and washed with 5% NaHCO₃ (3 x 25 mL). These aqueous washings were then taken to pH 1 and extracted with dichloromethane (3 x 25 mL). Evaporation of the organics *in vacuo* afforded 4.72 g of (1*R*,3*S*)-3-(methoxycarbonyl)cyclopentane-1-carboxylic acid (80 %, 99 % pure by GC-MS). ¹H NMR (300 MHz, CDCl₃) δ3.69, 2.88-2.80, 2.32-2.12, 2.03-1.93.

To argon flushed DCM (25 mL) was added 1.4 eq oxalyl chloride (0.81 mL, 9.40 mmol). The mixture was then transferred via cannula to a flask containing DMF (1 drop) and (1*R*,3*S*)-

(methoxycarbonyl)cyclopentane-1-carboxylic acid (1.08 g, 6.26 mmol) in DCM (17 mL) with vigorous stirring. Once the transfer was complete, the reaction was stirred for 2.5 hr under an argon atmosphere. Evaporation under reduced pressure yielded methyl (1*S*,3*R*)-3-(chlorocarbonyl)cyclopentane-1-carboxylate as a pale yellow oil (1.18 g, 99%) which was taken forward without further purification. ^1H NMR (300 MHz, CDCl_3) δ 3.69, 3.41-3.24, 2.92-2.81, 2.41-1.96.

Calculations:

Action spectra were calculated for neutral and anionic compound **1** using the following equation:²

$$j_\lambda = \left(\frac{2.303}{N_A} \right) \left(\frac{10^3 \text{ cm}^3}{L} \right) I_\lambda \varepsilon_\lambda \Phi_\lambda = (3.824E - 21) I_\lambda \varepsilon_\lambda \Phi_\lambda \quad (\text{S1})$$

where j_λ is the photolysis rate constant at wavelength λ , N_A is Avagadro's number, I_λ is the photon flux (photons /s /cm² /nm), ε_λ is the molar absorptivity (/M /cm /nm), and Φ_λ is the quantum yield (/nm) at wavelength λ . I_λ (Table S4) were obtained from the National Center for Atmospheric Research Quick TUV Calculator for Davis, CA during the midpoint of the outdoor exposure, August 29, 2017, at solar noon (1:00 PM PST).³

Simulated sunlight k_p values were converted to estimated outdoor values via the equation:

$$CF = \frac{j_{\text{sun}}}{j_{\text{solar_noon}}} = \frac{\frac{1}{24} \sum_{0}^{24} \sum_{290}^{340} j_{\text{per_h},\lambda}}{\sum_{290}^{340} j_{\text{solar_noon},\lambda}} = 0.283 \quad (\text{S2})$$

where j_{sun} (/s) is the 24-h average of the sum of j_λ (/s /nm) over 290 – 340 nm, or the predicted photolysis rate of compound **1** over 24 hours on August 29 2017, the midpoint day during outdoor exposure, and $j_{\text{solar_noon}}$ (/s) is the predicted photolysis rate of compound **1** at solar noon (1:00PM PST, August 29 2017), where the fastest photolysis rate will occur, as is the case for simulated sunlight experiments. The ratio of j_{sun} and $j_{\text{solar_noon}}$ allows for simulated sunlight compound **1** photolysis rates to be converted to estimated photolysis rates over 24 hours, approximating natural sunlight exposure.

To assess j_λ as a function of flood depth in a typical rice field, approximately 13 cm, light intensities were calculated for each cm of flood depth using the equation:

$$I_{l,\lambda} = I_{0,\lambda} e^{-\alpha_\lambda l} \quad (\text{S3})$$

where $I_{l,\lambda}$ is the light intensity at a certain depth in a flooded rice field at wavelength λ , $I_{0,\lambda}$ is the light intensity at the surface of a flooded rice field at wavelength λ (photon flux), α_λ is the attenuation coefficient at wavelength λ , and l is the flood depth (in cm). Attenuation coefficients were calculated thusly:

$$\alpha_\lambda = \frac{A_\lambda}{l_{cuvette}} \quad (\text{S4})$$

where A_λ is the absorbance of unfiltered rice field water at wavelength λ and $l_{cuvette}$ is the path length of the cuvette used for absorbance measurements (1 cm). The rate of anionic compound **1** photolysis, $j_{atten,\lambda}$, was then calculated using the derived average $I_{l,\lambda}$ values, from 0 – 13 cm depth, and photon flux, ε_λ , and Φ_λ values for anionic compound **1** in Table S2. A_λ for unfiltered rice field water, average $I_{l,\lambda}$, and $j_{atten,\lambda}$ values are given in Table S4.

Table S1. Molar absorptivities ($\epsilon_{\text{neutral},\lambda}$), quantum yields ($\Phi_{\text{neutral},\lambda}$), and calculated direct photolysis rates ($j_{\text{neutral},\lambda}$) for neutral compound **1**. Molar absorptivities were obtained as described in the Materials and Methods, quantum yields were derived using the equation for $\Phi_{\text{neutral},\lambda}$ vs. wavelength in Figure 2, and $j_{\text{neutral},\lambda}$ values were calculated using Equation S1.

Wavelength (nm)	$\epsilon_{\text{neutral},\lambda}$ (/M /cm /nm)	$\Phi_{\text{neutral},\lambda}$ (/nm)	Photon flux (photons /s /cm ² /nm)	$j_{\text{neutral},\lambda}$ (/s /nm)
400	0.00E+00	5.88E-03	4.18E+14	0.00E+00
399	0.00E+00	5.95E-03	3.97E+14	0.00E+00
398	3.55E-01	6.02E-03	3.81E+14	3.12E-09
397	0.00E+00	6.10E-03	2.21E+14	0.00E+00
396	0.00E+00	6.17E-03	1.91E+14	0.00E+00
395	6.22E+00	6.24E-03	3.25E+14	4.84E-08
394	5.33E+00	6.32E-03	2.52E+14	3.25E-08
393	1.71E-01	6.39E-03	1.07E+14	4.48E-10
392	0.00E+00	6.46E-03	2.46E+14	0.00E+00
391	0.00E+00	6.53E-03	3.27E+14	0.00E+00
390	3.78E+00	6.61E-03	2.76E+14	2.63E-08
389	5.23E+00	6.68E-03	2.80E+14	3.74E-08
388	4.69E+00	6.75E-03	2.22E+14	2.68E-08
387	5.48E+00	6.83E-03	2.21E+14	3.15E-08
386	3.99E+00	6.90E-03	2.37E+14	2.50E-08
385	5.44E+00	6.97E-03	2.32E+14	3.37E-08
384	4.29E+00	7.05E-03	2.34E+14	2.71E-08
383	3.58E+00	7.12E-03	1.56E+14	1.52E-08
382	1.16E+01	7.19E-03	1.77E+14	5.67E-08
381	1.02E+01	7.26E-03	2.65E+14	7.54E-08
380	8.93E+00	7.34E-03	2.82E+14	7.07E-08
379	9.34E+00	7.41E-03	2.34E+14	6.19E-08
378	1.03E+01	7.48E-03	3.16E+14	9.34E-08
377	9.64E+00	7.56E-03	2.89E+14	8.05E-08
376	1.42E+01	7.63E-03	2.42E+14	1.00E-07
375	1.38E+01	7.70E-03	2.42E+14	9.83E-08
374	1.23E+01	7.77E-03	2.14E+14	7.81E-08
373	2.09E+01	7.85E-03	1.95E+14	1.22E-07
372	2.25E+01	7.92E-03	2.15E+14	1.47E-07
371	2.14E+01	7.99E-03	2.91E+14	1.91E-07
370	2.19E+01	8.07E-03	2.54E+14	1.72E-07
369	2.53E+01	8.14E-03	2.79E+14	2.20E-07
368	2.97E+01	8.21E-03	2.33E+14	2.17E-07
367	3.57E+01	8.29E-03	2.64E+14	2.99E-07
366	3.40E+01	8.36E-03	2.78E+14	3.01E-07
365	3.48E+01	8.43E-03	2.62E+14	2.94E-07
364	4.43E+01	8.50E-03	2.15E+14	3.09E-07
363	4.82E+01	8.58E-03	1.96E+14	3.11E-07
362	5.01E+01	8.65E-03	2.20E+14	3.65E-07

361	5.72E+01	8.72E-03	1.87E+14	3.57E-07
360	6.24E+01	8.80E-03	2.07E+14	4.35E-07
359	7.00E+01	8.87E-03	2.23E+14	5.30E-07
358	8.07E+01	8.94E-03	1.32E+14	3.65E-07
357	8.81E+01	9.01E-03	1.71E+14	5.20E-07
356	9.12E+01	9.09E-03	2.01E+14	6.37E-07
355	9.29E+01	9.16E-03	2.16E+14	7.04E-07
354	1.03E+02	9.23E-03	2.31E+14	8.37E-07
353	1.12E+02	9.31E-03	2.13E+14	8.48E-07
352	1.28E+02	9.38E-03	1.77E+14	8.12E-07
351	1.44E+02	9.45E-03	1.95E+14	1.02E-06
350	1.52E+02	9.53E-03	2.26E+14	1.25E-06
349	1.69E+02	9.60E-03	1.61E+14	9.98E-07
348	1.83E+02	9.67E-03	1.92E+14	1.30E-06
347	1.92E+02	9.74E-03	1.74E+14	1.25E-06
346	2.03E+02	9.82E-03	1.78E+14	1.36E-06
345	2.23E+02	9.89E-03	1.90E+14	1.60E-06
344	2.50E+02	9.96E-03	1.38E+14	1.32E-06
343	2.70E+02	1.00E-02	1.97E+14	2.04E-06
342	2.86E+02	1.01E-02	1.89E+14	2.09E-06
341	3.15E+02	1.02E-02	1.71E+14	2.09E-06
340	3.54E+02	1.03E-02	1.91E+14	2.66E-06
339	3.85E+02	1.03E-02	1.79E+14	2.72E-06
338	4.26E+02	1.04E-02	1.64E+14	2.78E-06
337	4.59E+02	1.05E-02	1.55E+14	2.85E-06
336	4.97E+02	1.05E-02	1.41E+14	2.83E-06
335	5.46E+02	1.06E-02	1.80E+14	3.99E-06
334	6.01E+02	1.07E-02	1.77E+14	4.34E-06
333	6.63E+02	1.08E-02	1.58E+14	4.30E-06
332	7.29E+02	1.08E-02	1.68E+14	5.07E-06
331	7.98E+02	1.09E-02	1.69E+14	5.63E-06
330	8.72E+02	1.10E-02	1.71E+14	6.26E-06
329	9.54E+02	1.11E-02	1.88E+14	7.58E-06
328	1.04E+03	1.11E-02	1.44E+14	6.36E-06
327	1.13E+03	1.12E-02	1.55E+14	7.53E-06
326	1.24E+03	1.13E-02	1.67E+14	8.88E-06
325	1.35E+03	1.13E-02	1.36E+14	7.93E-06
324	1.46E+03	1.14E-02	1.21E+14	7.72E-06
323	1.58E+03	1.15E-02	1.03E+14	7.13E-06
322	1.72E+03	1.16E-02	9.80E+13	7.44E-06
321	1.86E+03	1.16E-02	9.82E+13	8.15E-06
320	2.01E+03	1.17E-02	1.14E+14	1.03E-05
319	2.18E+03	1.18E-02	9.27E+13	9.11E-06
318	2.36E+03	1.19E-02	7.55E+13	8.08E-06
317	2.55E+03	1.19E-02	9.40E+13	1.10E-05
316	2.76E+03	1.20E-02	6.63E+13	8.40E-06
315	2.98E+03	1.21E-02	6.51E+13	8.97E-06
314	3.21E+03	1.22E-02	6.25E+13	9.34E-06
313	3.46E+03	1.22E-02	6.08E+13	9.83E-06

312	3.73E+03	1.23E-02	5.30E+13	9.31E-06
311	4.00E+03	1.24E-02	5.25E+13	9.95E-06
310	4.28E+03	1.24E-02	4.00E+13	8.14E-06
309	4.59E+03	1.25E-02	2.85E+13	6.25E-06
308	4.91E+03	1.26E-02	3.10E+13	7.33E-06
307	5.26E+03	1.27E-02	2.70E+13	6.88E-06
306	5.64E+03	1.27E-02	1.77E+13	4.85E-06
305	6.02E+03	1.28E-02	1.64E+13	4.83E-06
304	6.43E+03	1.29E-02	1.15E+13	3.66E-06
303	6.87E+03	1.30E-02	1.01E+13	3.42E-06
302	7.33E+03	1.30E-02	5.44E+12	1.99E-06
301	7.82E+03	1.31E-02	4.08E+12	1.60E-06
300	8.32E+03	1.32E-02	1.86E+12	7.80E-07
299	8.82E+03	1.32E-02	1.81E+12	8.09E-07
298	9.29E+03	1.33E-02	7.21E+11	3.41E-07
297	9.75E+03	1.34E-02	5.35E+11	2.67E-07
296	1.02E+04	1.35E-02	2.41E+11	1.26E-07
295	1.06E+04	1.35E-02	1.17E+11	6.43E-08
294	1.10E+04	1.36E-02	3.83E+10	2.20E-08
293	1.14E+04	1.37E-02	1.67E+10	9.98E-09
292	1.17E+04	1.38E-02	4.58E+09	2.82E-09
291	1.20E+04	1.38E-02	1.48E+09	9.41E-10
290	1.23E+04	1.39E-02	0.00E+00	0.00E+00

Table S2. Molar absorptivities ($\epsilon_{\text{anionic}, \lambda}$), quantum yields ($\Phi_{\text{anionic}, \lambda}$), and calculated direct photolysis rates ($j_{\text{anionic}, \lambda}$) for anionic compound **1**. Molar absorptivities were obtained as described in the Materials and Methods, quantum yields were derived using the equation for $\Phi_{\text{anionic}, \lambda}$ vs. wavelength in Figure 2, and $j_{\text{anionic}, \lambda}$ values were calculated using Equation S1.

Wavelength (nm)	$\epsilon_{\text{anionic}, \lambda}$ (/M /cm /nm)	$\Phi_{\text{anionic}, \lambda}$ (/nm)	Photon flux (photons /s /cm ² /nm)	$j_{\text{anionic}, \lambda}$ (/s /nm)
400	2.38E+01	0.00E+00	4.18E+14	0.00E+00
399	2.41E+01	0.00E+00	3.97E+14	0.00E+00
398	2.65E+01	0.00E+00	3.81E+14	0.00E+00
397	3.00E+01	0.00E+00	2.21E+14	0.00E+00
396	3.41E+01	0.00E+00	1.91E+14	0.00E+00
395	3.81E+01	0.00E+00	3.25E+14	0.00E+00
394	3.98E+01	0.00E+00	2.52E+14	0.00E+00
393	4.24E+01	0.00E+00	1.07E+14	0.00E+00
392	4.80E+01	0.00E+00	2.46E+14	0.00E+00
391	5.40E+01	0.00E+00	3.27E+14	0.00E+00
390	5.86E+01	0.00E+00	2.76E+14	0.00E+00
389	6.28E+01	0.00E+00	2.80E+14	0.00E+00
388	6.33E+01	0.00E+00	2.22E+14	0.00E+00
387	6.82E+01	0.00E+00	2.21E+14	0.00E+00
386	7.50E+01	0.00E+00	2.37E+14	0.00E+00
385	7.81E+01	0.00E+00	2.32E+14	0.00E+00
384	8.65E+01	0.00E+00	2.34E+14	0.00E+00
383	9.30E+01	0.00E+00	1.56E+14	0.00E+00
382	9.85E+01	0.00E+00	1.77E+14	0.00E+00
381	1.03E+02	0.00E+00	2.65E+14	0.00E+00
380	1.11E+02	0.00E+00	2.82E+14	0.00E+00
379	1.18E+02	0.00E+00	2.34E+14	0.00E+00
378	1.26E+02	0.00E+00	3.16E+14	0.00E+00
377	1.37E+02	0.00E+00	2.89E+14	0.00E+00
376	1.49E+02	0.00E+00	2.42E+14	0.00E+00
375	1.59E+02	0.00E+00	2.42E+14	0.00E+00
374	1.69E+02	0.00E+00	2.14E+14	0.00E+00
373	1.83E+02	0.00E+00	1.95E+14	0.00E+00
372	1.96E+02	0.00E+00	2.15E+14	0.00E+00
371	2.07E+02	0.00E+00	2.91E+14	0.00E+00
370	2.19E+02	0.00E+00	2.54E+14	0.00E+00
369	2.38E+02	0.00E+00	2.79E+14	0.00E+00
368	2.59E+02	0.00E+00	2.33E+14	0.00E+00
367	2.73E+02	0.00E+00	2.64E+14	0.00E+00
366	2.94E+02	0.00E+00	2.78E+14	0.00E+00
365	3.19E+02	0.00E+00	2.62E+14	0.00E+00
364	3.38E+02	0.00E+00	2.15E+14	0.00E+00
363	3.60E+02	0.00E+00	1.96E+14	0.00E+00
362	3.90E+02	0.00E+00	2.20E+14	0.00E+00
361	4.13E+02	0.00E+00	1.87E+14	0.00E+00

360	4.36E+02	0.00E+00	2.07E+14	0.00E+00
359	4.69E+02	0.00E+00	2.23E+14	0.00E+00
358	5.02E+02	0.00E+00	1.32E+14	0.00E+00
357	5.37E+02	0.00E+00	1.71E+14	0.00E+00
356	5.68E+02	0.00E+00	2.01E+14	0.00E+00
355	6.01E+02	0.00E+00	2.16E+14	0.00E+00
354	6.45E+02	0.00E+00	2.31E+14	0.00E+00
353	6.96E+02	0.00E+00	2.13E+14	0.00E+00
352	7.38E+02	0.00E+00	1.77E+14	0.00E+00
351	7.73E+02	0.00E+00	1.95E+14	0.00E+00
350	8.19E+02	0.00E+00	2.26E+14	0.00E+00
349	8.71E+02	0.00E+00	1.61E+14	0.00E+00
348	9.25E+02	0.00E+00	1.92E+14	0.00E+00
347	9.80E+02	0.00E+00	1.74E+14	0.00E+00
346	1.04E+03	0.00E+00	1.78E+14	0.00E+00
345	1.10E+03	0.00E+00	1.90E+14	0.00E+00
344	1.15E+03	0.00E+00	1.38E+14	0.00E+00
343	1.21E+03	0.00E+00	1.97E+14	0.00E+00
342	1.28E+03	0.00E+00	1.89E+14	0.00E+00
341	1.36E+03	0.00E+00	1.71E+14	0.00E+00
340	1.43E+03	0.00E+00	1.91E+14	0.00E+00
339	1.51E+03	0.00E+00	1.79E+14	0.00E+00
338	1.60E+03	0.00E+00	1.64E+14	0.00E+00
337	1.69E+03	0.00E+00	1.55E+14	0.00E+00
336	1.78E+03	3.71E-06	1.41E+14	3.55E-09
335	1.87E+03	4.64E-05	1.80E+14	5.99E-08
334	1.97E+03	8.80E-05	1.77E+14	1.17E-07
333	2.08E+03	1.28E-04	1.58E+14	1.61E-07
332	2.18E+03	1.67E-04	1.68E+14	2.34E-07
331	2.28E+03	2.05E-04	1.69E+14	3.03E-07
330	2.39E+03	2.42E-04	1.71E+14	3.79E-07
329	2.51E+03	2.78E-04	1.88E+14	5.02E-07
328	2.64E+03	3.12E-04	1.44E+14	4.51E-07
327	2.75E+03	3.45E-04	1.55E+14	5.64E-07
326	2.88E+03	3.77E-04	1.67E+14	6.93E-07
325	3.01E+03	4.08E-04	1.36E+14	6.37E-07
324	3.14E+03	4.37E-04	1.21E+14	6.36E-07
323	3.27E+03	4.66E-04	1.03E+14	6.01E-07
322	3.43E+03	4.93E-04	9.80E+13	6.33E-07
321	3.58E+03	5.19E-04	9.82E+13	6.97E-07
320	3.74E+03	5.44E-04	1.14E+14	8.84E-07
319	3.91E+03	5.67E-04	9.27E+13	7.86E-07
318	4.08E+03	5.89E-04	7.55E+13	6.95E-07
317	4.27E+03	6.11E-04	9.40E+13	9.37E-07
316	4.45E+03	6.30E-04	6.63E+13	7.12E-07
315	4.65E+03	6.49E-04	6.51E+13	7.51E-07
314	4.85E+03	6.67E-04	6.25E+13	7.74E-07
313	5.08E+03	6.83E-04	6.08E+13	8.07E-07
312	5.32E+03	6.98E-04	5.30E+13	7.54E-07

311	5.56E+03	7.12E-04	5.25E+13	7.95E-07
310	5.80E+03	7.25E-04	4.00E+13	6.43E-07
309	6.05E+03	7.36E-04	2.85E+13	4.86E-07
308	6.33E+03	7.47E-04	3.10E+13	5.61E-07
307	6.63E+03	7.56E-04	2.70E+13	5.18E-07
306	6.94E+03	7.64E-04	1.77E+13	3.58E-07
305	7.28E+03	7.71E-04	1.64E+13	3.51E-07
304	7.62E+03	7.76E-04	1.15E+13	2.61E-07
303	7.97E+03	7.80E-04	1.01E+13	2.39E-07
302	8.32E+03	7.84E-04	5.44E+12	1.36E-07
301	8.70E+03	7.85E-04	4.08E+12	1.07E-07
300	9.07E+03	7.86E-04	1.86E+12	5.07E-08
299	9.42E+03	7.86E-04	1.81E+12	5.12E-08
298	9.74E+03	7.84E-04	7.21E+11	2.11E-08
297	1.00E+04	7.81E-04	5.35E+11	1.60E-08
296	1.03E+04	7.77E-04	2.41E+11	7.39E-09
295	1.05E+04	7.72E-04	1.17E+11	3.65E-09
294	1.07E+04	7.65E-04	3.83E+10	1.20E-09
293	1.09E+04	7.58E-04	1.67E+10	5.30E-10
292	1.11E+04	7.49E-04	4.58E+09	1.45E-10
291	1.12E+04	7.39E-04	1.48E+09	4.67E-11
290	1.12E+04	7.27E-04	0.00E+00	0.00E+00

Table S3. Absorbances (A_λ) and screening factors for rice field water and Sacramento River water filtered to 0.2 μm . Screening factors for samples irradiated with simulated sunlight are denoted as $S_{SS,\lambda}$ and screening factors for samples exposed to natural sunlight are denoted as $S_{NS,\lambda}$. Wavelengths were selected in reference to the range of non-zero $j_{anionic,\lambda}$ values (Table S2).

Wavelength (nm)	Rice field water (filtered)			Sacramento River water (filtered)		
	A_λ (/nm)	$S_{SS,\lambda}$ (/nm)	$S_{NS,\lambda}$ (/nm)	A_λ (/nm)	$S_{SS,\lambda}$ (/nm)	$S_{NS,\lambda}$ (/nm)
340	0.057	0.879	0.925	0.0101	0.977	0.986
339	0.0584	0.877	0.923	0.0106	0.976	0.985
338	0.0592	0.875	0.922	0.0109	0.975	0.985
337	0.0599	0.874	0.921	0.0111	0.975	0.985
336	0.061	0.872	0.920	0.0114	0.974	0.984
335	0.0623	0.869	0.918	0.0111	0.975	0.985
334	0.0634	0.867	0.917	0.0111	0.975	0.985
333	0.0641	0.866	0.916	0.0114	0.974	0.984
332	0.0647	0.865	0.916	0.0115	0.974	0.984
331	0.0656	0.863	0.914	0.0118	0.973	0.984
330	0.067	0.860	0.913	0.0116	0.974	0.984
329	0.0687	0.857	0.911	0.0121	0.972	0.983
328	0.0704	0.854	0.909	0.0126	0.971	0.983
327	0.0716	0.852	0.907	0.0128	0.971	0.982
326	0.0723	0.850	0.906	0.0133	0.970	0.982
325	0.0735	0.848	0.905	0.0132	0.970	0.982
324	0.0749	0.846	0.903	0.0132	0.970	0.982
323	0.0759	0.844	0.902	0.0134	0.970	0.982
322	0.0771	0.842	0.900	0.0136	0.969	0.981
321	0.0786	0.839	0.899	0.0137	0.969	0.981
320	0.0801	0.836	0.897	0.014	0.968	0.981
319	0.0817	0.833	0.895	0.0144	0.967	0.980
318	0.083	0.831	0.893	0.015	0.966	0.979
317	0.0843	0.829	0.892	0.0155	0.965	0.979
316	0.0855	0.826	0.890	0.0156	0.965	0.979
315	0.0867	0.824	0.889	0.0157	0.965	0.978
314	0.0881	0.822	0.887	0.0159	0.964	0.978
313	0.0897	0.819	0.886	0.0162	0.963	0.978
312	0.0912	0.816	0.884	0.0166	0.963	0.977
311	0.0925	0.814	0.882	0.0167	0.962	0.977
310	0.0939	0.812	0.881	0.0164	0.963	0.978
309	0.0954	0.809	0.879	0.0169	0.962	0.977
308	0.0974	0.806	0.877	0.0178	0.960	0.976
307	0.0989	0.803	0.875	0.0181	0.959	0.975
306	0.1004	0.801	0.873	0.0184	0.959	0.975

305	0.1022	0.797	0.871	0.0186	0.958	0.975
304	0.104	0.794	0.869	0.0191	0.957	0.974
303	0.1058	0.791	0.867	0.0198	0.956	0.973
302	0.1077	0.788	0.865	0.0205	0.954	0.972
301	0.1099	0.785	0.862	0.0207	0.954	0.972
300	0.1121	0.781	0.860	0.0209	0.953	0.971
299	0.114	0.778	0.858	0.021	0.953	0.971
298	0.1161	0.774	0.855	0.0213	0.952	0.971
297	0.1183	0.771	0.853	0.022	0.951	0.970
296	0.1207	0.767	0.850	0.0228	0.949	0.969
295	0.1232	0.763	0.847	0.0237	0.947	0.968
294	0.126	0.759	0.844	0.0239	0.947	0.968
293	0.1283	0.755	0.842	0.0241	0.946	0.967
292	0.1304	0.752	0.840	0.0248	0.945	0.966
291	0.1327	0.748	0.837	0.0255	0.943	0.965
290	0.1351	0.744	0.834	0.0259	0.942	0.965

Table S4. Unfiltered rice field water absorbances (A_{λ}), photon flux ($I_{0,\lambda}$) at solar noon at the median day samples were exposed to natural light, August 29, 2017, as determined by TUV calculator,³ average photon flux as over the typical depth flooding in a rice field (13 cm), and estimated attenuated compound **1** photolysis rates ($j_{atten,\lambda}$) calculated using average $I_{l,\lambda}$ values (Equation S1).

λ (nm)	A_{λ} (/nm)	$I_{0,\lambda}$ (photons /s /cm ² /nm)	Avg. $I_{l,\lambda}$ (photons /s /cm ² /nm)	$j_{atten,\lambda}$ (/s /nm)
340	0.0725	1.79E+14	1.16E+14	0.00E+00
339	0.0736	1.64E+14	1.06E+14	0.00E+00
338	0.0748	1.55E+14	9.94E+13	0.00E+00
337	0.0758	1.41E+14	9.01E+13	0.00E+00
336	0.0766	1.80E+14	1.15E+14	2.89E-09
335	0.0774	1.77E+14	1.12E+14	3.73E-08
334	0.0788	1.58E+14	9.92E+13	6.58E-08
333	0.0802	1.68E+14	1.05E+14	1.07E-07
332	0.0814	1.69E+14	1.05E+14	1.46E-07
331	0.0823	1.71E+14	1.06E+14	1.89E-07
330	0.0835	1.88E+14	1.15E+14	2.56E-07
329	0.0851	1.44E+14	8.74E+13	2.33E-07
328	0.0865	1.55E+14	9.38E+13	2.95E-07
327	0.0878	1.67E+14	1.00E+14	3.64E-07
326	0.0891	1.36E+14	8.10E+13	3.37E-07
325	0.0903	1.21E+14	7.19E+13	3.37E-07
324	0.0912	1.03E+14	6.08E+13	3.19E-07
323	0.0923	9.80E+13	5.75E+13	3.35E-07
322	0.0936	9.82E+13	5.73E+13	3.70E-07
321	0.0949	1.14E+14	6.58E+13	4.67E-07
320	0.0963	9.27E+13	5.33E+13	4.15E-07
319	0.0979	7.55E+13	4.31E+13	3.65E-07
318	0.0994	9.40E+13	5.33E+13	4.90E-07
317	0.1007	6.63E+13	3.73E+13	3.72E-07
316	0.1024	6.51E+13	3.63E+13	3.90E-07
315	0.104	6.25E+13	3.46E+13	3.99E-07
314	0.1053	6.08E+13	3.34E+13	4.14E-07
313	0.1067	5.30E+13	2.90E+13	3.85E-07
312	0.108	5.25E+13	2.85E+13	4.05E-07
311	0.1096	4.00E+13	2.15E+13	3.26E-07
310	0.1111	2.85E+13	1.52E+13	2.45E-07
309	0.1122	3.10E+13	1.65E+13	2.82E-07
308	0.114	2.70E+13	1.43E+13	2.58E-07
307	0.116	1.77E+13	9.23E+12	1.77E-07
306	0.1178	1.64E+13	8.48E+12	1.72E-07

305	0.1196	1.15E+13	5.93E+12	1.27E-07
304	0.1214	1.01E+13	5.12E+12	1.16E-07
303	0.1232	5.44E+12	2.75E+12	6.54E-08
302	0.1252	4.08E+12	2.04E+12	5.10E-08
301	0.127	1.86E+12	9.24E+11	2.41E-08
300	0.129	1.81E+12	8.91E+11	2.43E-08
299	0.131	7.21E+11	3.52E+11	9.96E-09
298	0.1335	5.35E+11	2.58E+11	7.53E-09
297	0.1363	2.41E+11	1.15E+11	3.45E-09
296	0.1385	1.17E+11	5.53E+10	1.69E-09
295	0.1406	3.83E+10	1.79E+10	5.57E-10
294	0.1433	1.67E+10	7.73E+09	2.43E-10
293	0.146	4.58E+09	2.09E+09	6.62E-11
292	0.1484	1.48E+09	6.69E+08	2.12E-11
291	0.151	0.00E+00	0.00E+00	0.00E+00
290	0.1536	0.00E+00	0.00E+00	0.00E+00

Table S5. TUV Calculator Parameter Inputs For Davis, CA.³ Output Option 1 (Actinic Flux, Spectral) was Selected For All Actinic Flux Measurements.

Parameter	Value
λ start (nm)	280
λ end (nm)	420
Increments	140
Latitude (deg)	38.5449
Longitude (deg)	-121.740
Overhead ozone column (du)	300
Surface albedo	0.1
Ground elevation (km asl)	0.016
Measurement altitude (km asl)	0.03
Direct beam	1.0
Diffuse down	1.0
Diffuse up	1.0

Table S6. PFAM Inputs for Application of Benzobicyclon (BZB) on a Typical California Rice Field.

Parameter	Benzobicyclon	Compound 1	Ratio compound 1 : benzobicyclon (mol)
K _{oc} (mL /g) ^{1, 4}	27900	954.99	-
Water Column half-life (d) (Temp, °C)	1E8* (25)	274 [‡] (25)	0
Benthic (anaerobic) half-life (d) ¹ (Temp, °C)	1E8* (20)	986.4 [‡] (24)	0
Aerobic half-life (d) ¹ (Temp, °C)	1E8* (20)	411 [‡] (24)	0
Near surface photolysis half-life (d) Latitude (°)	1E8* 40	7.4 40	0
Hydrolysis half-life (d) ⁵	0.667	1E8*	1
Molecular weight (g/mol)	446.97	354.805	-
Vapor pressure (torr)	1.00E-09*	1.00E-15*	-
Aqueous solubility (g/mL)	5.00E-09	1.46E-04	-
Heat of Henry (J/mol) (Temp, °C)	1000000* (20)	1000000* (20)	-
Date field flooded	May 5	-	-
Date applied	May 15	-	-
Mass applied (kg/ha)	0.3027	-	-
Slow release (/d) [†]	0.33	-	-
Drift factor	0	-	-

*Value has not been experimentally determined and/or is estimated to be a minor contributor to compound 1 fate for the purpose of this study.

[†]Estimated using commercial thiobencarb granule formulation data provided by Hussain *et al.*⁶

[‡]Determined using experimental half-life multiplied by 2 (Water Column half-life) or 3 (Benthic and Aerobic half-lives) as only one experimental value was available.⁷

Table S7. Unscreened Photolysis Rates and Half-Lives for Compound **1** in Natural Waters

Treatment	Parameter	Simulated sunlight			
		Summer solstice (midday)	Fall equinox (midday)	Fall equinox (24-h equivalent)*	Natural sunlight [†]
Filtered Rice field water	j_p (/h)	0.052 (0.003)	0.044 (0.002)	0.013 (0.001)	0.0077 (0.0007)
	$t_{1/2}$ (h)	13 (\pm 1)	16 (\pm 1)	56 (\pm 3)	91 (\pm 2)
Filtered Sacramento River water	j_p (/h)	0.024 (0.001)	0.021 (0.001)	0.0058 (0.001)	0.0033 (0.0001)
	$t_{1/2}$ (h)	29 (\pm 1)	34 (\pm 1)	120 (\pm 3)	210 (\pm 3)

*Value estimated by converting simulated sunlight photolysis result from lab to photolysis via natural sunlight using the 24-hour conversion factor of 0.283 (Equation S2).

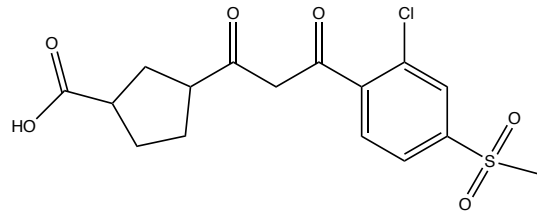


Figure S1. Chemical structure of 3-{3-[2-chloro-4-(methanesulfonyl)phenyl]-3-oxopropanoyl)cyclopentane-1-carboxylic acid

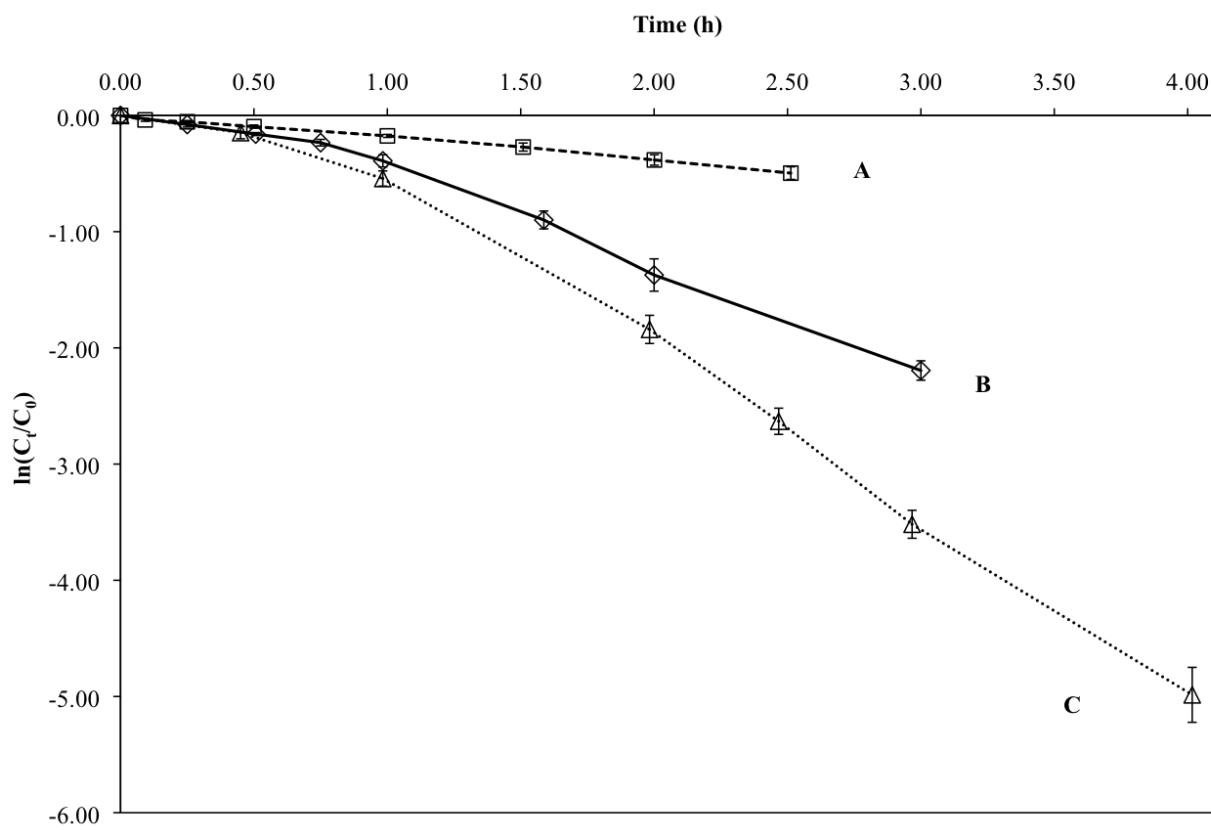


Figure S2. Photolysis of neutral compound **1** in (A) simulated sunlight with 25 μM isopropanol, (B) simulated sunlight without isopropanol, and (C) natural sunlight with 25 μM isopropanol. Error bars represent standard error ($n = 3$).

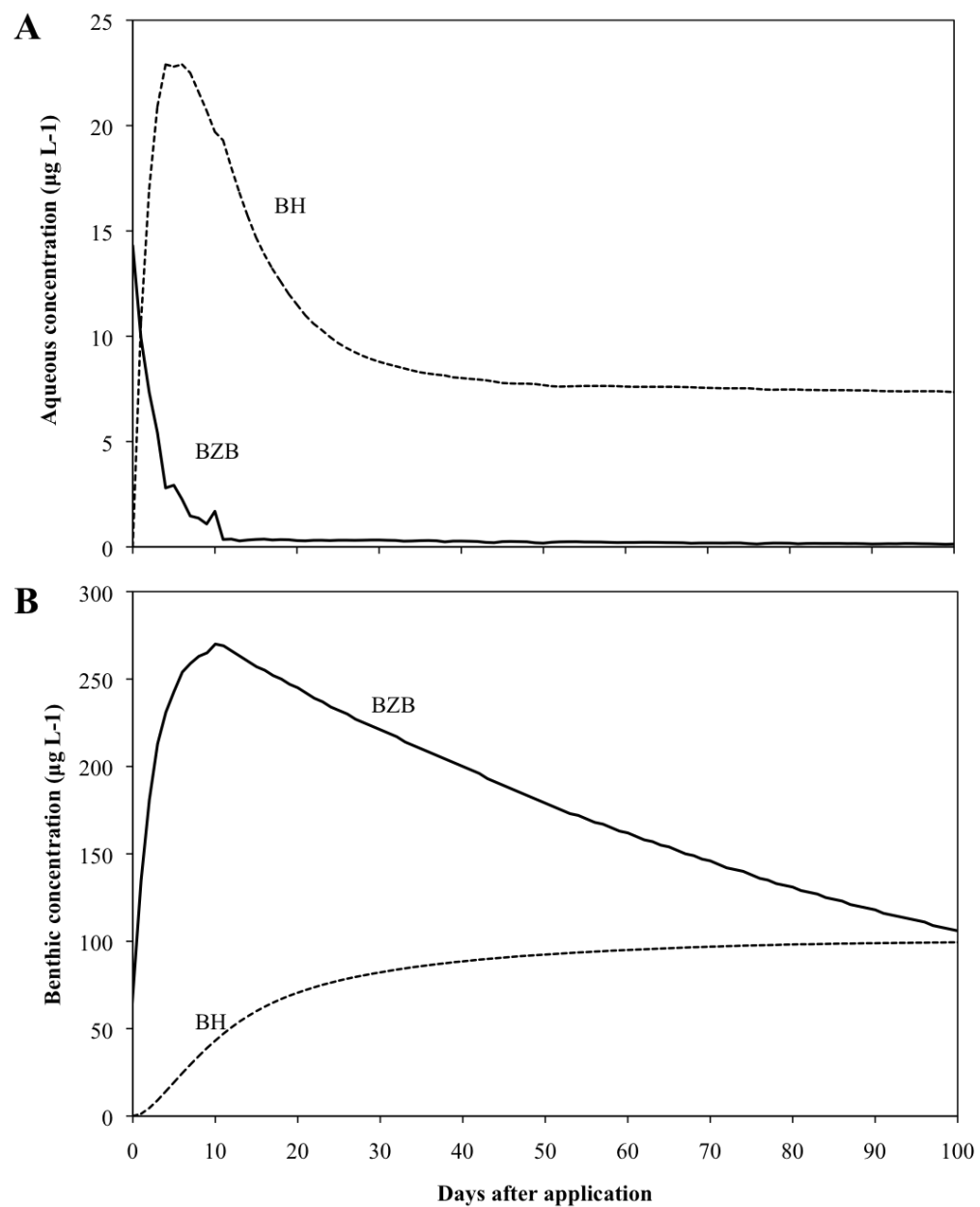


Figure S3. Concentration of benzobicyclon (solid line) and benzobicyclon hydrolysate (compound 1 ; dashed line) predicted by PFAM in the (A) aqueous fraction and (B) benthic fraction in a flooded model rice field following application of benzobicyclon at 0.303 kg/ha.

References

1. Williams, K. L.; Gladfelder, J. J.; Quigley, L. L.; Ball, D. B.; Tjeerdema, R. S., Dissipation of the herbicide benzobicyclon hydrolysate in a model California rice field soil. *J. Agric. Food Chem.* **2017**, *65*, 9200-9207.
2. Leifer, A., *The kinetics of environmental aquatic photochemistry: Theory and practice*. American Chemical Society: Washington, DC, 1988.
3. National Center for Atmospheric Research Atmospheric Chemistry Observations & Modeling. Quick TUV Calculator. http://cprm.acom.ucar.edu/Models/TUV/Interactive_TUV/ (accessed October 20, 2017).
4. *Estimation Programs Interface Suite™ for Microsoft® windows*, v 4.11; United States Environmental Protection Agency: Washington DC, USA, 2015.
5. Williams, K. L.; Tjeerdema, R. S., Hydrolytic activation kinetics of the herbicide benzobicyclon in simulated aquatic systems. *J. Agric. Food Chem.* **2016**, *64*, 4838-4844.
6. Hussain, M.; Gant, J.; Rathor, M. N., Preparation of controlled-release formulations of ¹⁴C-labelled thiobencarb herbicide and study of their environmental behaviour. *Pestic. Sci.* **1992**, *34*, 341-347.
7. USEPA. *Guidance for Selecting Input Parameters for the Pesticide in Flooded Applications Model (PFAM)*; United States Environmental Protection Agency: Washington DC, USA, 2016.